Reflectarray Design for 120-GHz MMID Application: Simulation Results

A. Tamminen[1], J. Ala-Laurinaho[1], J. Häkli[2], P. Koivisto[2], J. Säily[2], A. Luukanen[2], A. V. Räisänen[1]
[1]MilliLab/SMARAD, Aalto University Department of Radio Science and Engineering
Otakaari 5 A, 00076 Aalto, Finland
aleksi.tamminen@aalto.fi
[2]MilliLab, VTT Technical Research Centre of Finland
Tietotie 3, 02150 Espoo, Finland

***Abstract*- We present simulation results for a reconfigurable reflectarray designed for MMID and imaging applications at 120 GHz. The reflectarray is based on 4-state phase-modulating elements. Reflectarray design principle and optimized phase patterns are presented. Array element design, phase shifting properties, element efficiency, and effect of manufacturing errors are simulated. Also, piecewise assembled reflectarray is considered.**

I. INTRODUCTION

A reflectarray can be used to replace a conventional reflector used in a millimeter-wave antenna system. It consists of an array of reflecting elements, which modulate the reflected field in amplitude or phase in order to create a desired beam. A reflectarray is considered to have advantages over conventional designs due to its flatness and to the flexibility to form a variety of beam shapes with relative simple reflecting elements, such as microstrip-based patch antennas coupled to phase shifters [1]. The beam can also be actively steered, if the phase shift from the elements can be individually controlled. Reconfigurable reflectarrays have been designed for use at millimeter wavelengths in [2] and [3].

At Aalto University Department of Radio Science and Engineering and at Technical Research Centre of Finland (VTT), a 120-GHz reflectarray is being developed. The 140-mm reflectarray is suitable for use in, e.g., millimeter-wave identification (MMID) or imaging application. The reflectarray will consist of about 3700 patch antennas coupled to micro-electro-mechanical-system (MEMS) -based phase shifters, which are individually computer controlled. The phase shifters induce 0°, 90°, 180°, and 270° relative phase shifts. A sketch of the reflectarray system is shown in Fig. 1.

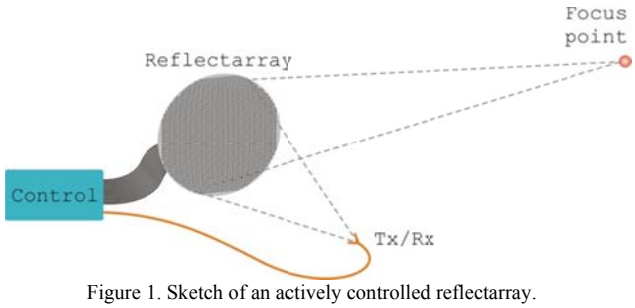

Figure 1. Sketch of an actively controlled reflectarray.

II. REFLECTARRAY DESIGN

As a preliminary study perceiving the actively controlled system, static reflectarrays are designed and will be manufactured. Different test schemes will cover focusing the beam to a certain distance and to certain offset from boresight.

The array will be produced on a 150-mm silicon wafer. The elements are equi-spaced with 2-mm separation and are connected to 4-state phase shifters. Discrete phase shift reduces reflectarray directivity about 1 dB compared to phase shifters with continuous phase shift. The element separation allows beam steering up to 38 degrees from normal.

The reflectarray is illuminated with a corrugated horn antenna positioned at 300-mm distance and 150-mm offset from the center of the reflectarray (Fig. 2). The horn provides Gaussian beam, and its center coincides with that of the reflectarray. The corrugated horn antenna provides −8…−9 -dB edge taper on the reflectarray. In simulations, the feed antenna is modeled by a Gaussian amplitude distribution and by a spherical phase front.

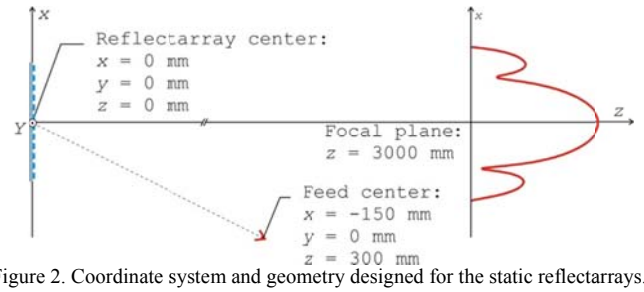

Figure 2. Coordinate system and geometry designed for the static reflectarrays.

Reflectarray Design Principle

The reflectarray is designed to modulate the phase of the reflected field. The design goal is to produce a constructive interference at the desired focusing point. In order to have constructive interference at the focus, (x_{fo}, y_{fo}, z_{fo}), of the reflectarray a phase shift needed is:

$$\varphi_{i,j} = \frac{2\pi}{\lambda}\left(R_{i,j} - R_{ref.}\right) mod\ 2\pi, \qquad (1)$$

where, $R_{i,j}$ is the total distance from the feed to an element (i,j) and from the element to the focus at the target. Term $R_{ref.}$ is the reference distance, e.g., related to the center element, against which all the elements are compared. In the

reflectarray, continuous phase from Eq. (1) are mapped in to four values. The mapping algorithm is:

$$\phi_{i,j} = \begin{cases} 0°, \ \varphi_{i,j} \in [-45°, 45°) \\ 90°, \ \varphi_{i,j} \in [45°,135°) \\ 180°, \ \varphi_{i,j} \in [135°,225°) \\ 270°, \ \varphi_{i,j} \in [225°,315°) \end{cases}. \quad (2)$$

The required phase shift is calculated either from Eq. (1) or by using a genetic algorithm (GA) developed in house. GA optimisers are robust, stochastic search methods, nowadays increasingly used in electromagnetics [4-6]. As a global optimiser, GA is suitable for decreasing the possibility that the optimisation sticks in a local minimum. GA is initially developed to optimise binary parameters, thus it goes well with the optimisation of discrete valued phase shifts.

In reflectarray optimization, GA is used to solve the inverse problem for the calculation of the electric field radiated by a given phase delays at the elements. Three different ways to calculate the field have been presented in the literature [7-10].

We have generalized the formula given in [7, 8]. In our generalized formula, vector form of all the fields; that of the feed, the antenna element, and the radiated electromagnetic field, are used. The components of the vector fields for the array elements are calculated using a spherical wave expansion (SWE). In addition to the phase delays for the array elements, also a different amplitude attenuation corresponding to each phase delay state for the phase shifter is included in the generalized formula. The field radiated by each element is multiplied by the corresponding phase-shift and amplitude - factor, and finally all of them at same point are added together to produce the radiated field. The generalized formula is applicable also when the array elements are located in the near-field region of the feed antenna. Also the field point itself can be located in the near-field region of the reflectarray. Both the original and our generalized equation give only the part of the total field, which is radiated by the reflectarray elements. Thus, the fields caused by reflection and edge diffraction as well as the field passing the array are ignored.

The initial generation for the GA optimisation is generated. One member, i.e., a set of the phase shifts is obtained using Eq. (1). The second member is obtained by adding to Eq. (1) the phase of each array elements radiation pattern in the feed direction. In this way, also the radiation pattern of the array elements is taken into account. Several solutions to the initial generation are obtained by demanding constant phase of the fields at the targeted focus. This method takes into account the radiation pattern of the element at the focus. The shortcoming of all these procedures is that the phase shift in reality should be a continuous function, while here a discrete set of phase shifts must be found. Allowing the phase to be discrete by approximating each phase shift by the nearest allowable value provides a useful approximation.

An optimal phase delay pattern for the circular reflectarray is calculated using GA. Out of the 150-mm wafer only circle with 140 mm diameter is filled with the element antennas. Thus total 3713 elements are included in the reflectarray.The phase shifters are expected to be lossy and attenuation, relative to shorted stub, of 0.8 dB is taken into account with open-ended stub The optimal phase delay patterns are calculated for focus at $x = 0$ mm and $x = 500$ mm with $y = 0$ mm and $z = 3000$ mm. The results calculated by GA are shown in Fig. 3. Compared to the solution given by Eq. (1) the GA optimization leads to solution where 4.2 % ($x = 0$ mm) and 8.2 % ($x = 500$ mm) of the phase shifters are in different state (90° difference). Compared to the analytical solution of Eq. 1, the power at the aimed focus increases only a fraction of decibel with solution from GA. Depending on the transversal focus position, the peak power occurs with accuracy of 0.3 mm or 0.5-0.8 mm with solution from GA or Eq. 1, respectively. Fig. 4 shows the relative power obtained by GA optimization at the x-cut with $z = 3000$ mm and $y = 0$ mm. This figure reveals good agreement of the peak power in the targeted focus point. The 3-dB beamwidth is 60 mm at distance $z = 3000$ mm.

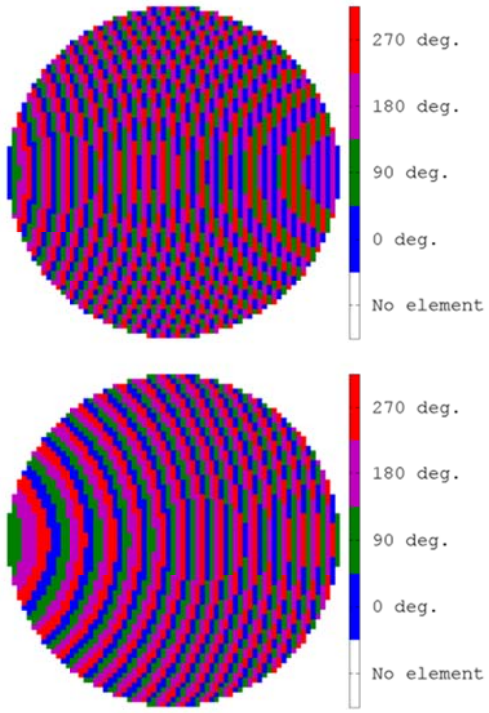

Figure 3. Optimized phase shift patterns for array with focus at $y = 0$ mm, $z = 3000$ mm and a) $x = 0$ mm b) $x = 500$ mm.

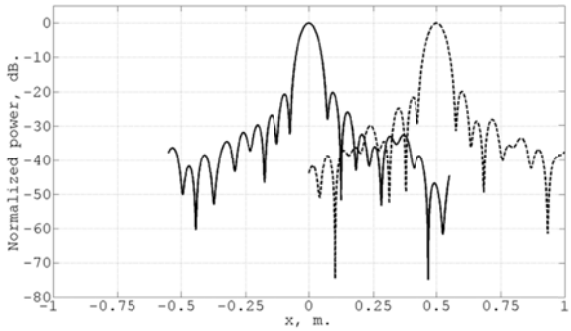

Figure 4. Beams focused at 3000 mm to $x = 0$ mm (solid line) and to $x = 500$ mm (dashed line).

Reflectarray Element and Phase Shifters

The static reflectarray elements are based on grounded coplanar waveguide (GCPW) patch antennas coupled to a stub with length according to the desired phase shift. Both open-ended and shorted stubs are used. The reconfigurability can be achieved by replacing the stubs with active MEMS switch structure. Fig. 5 shows a single reflectarray element with open-ended stub. The element directional pattern is presented in Fig. 6.

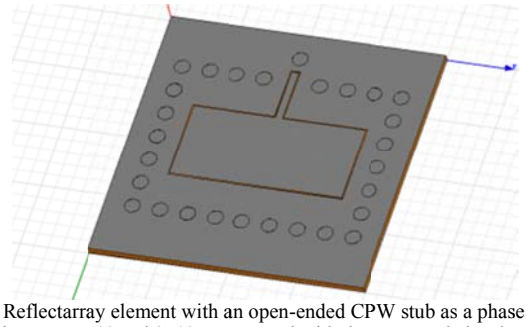

Figure 5. Reflectarray element with an open-ended CPW stub as a phase shifter. Phase states 0° and 270° are covered with the open-ended stub.

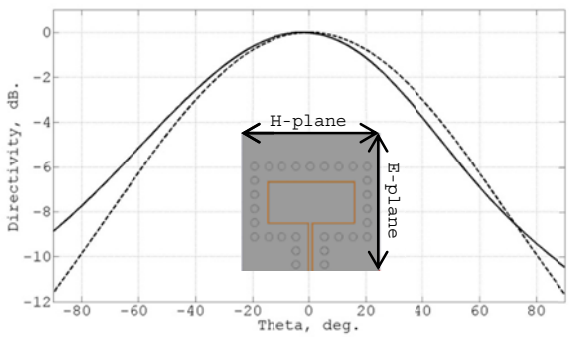

Figure 6. E- (solid line) and H-cuts (dashed line) of the element directional pattern.

The 1.25-mm by 0.585-mm GCPW patch antenna has 50-µm thick polyimide substrate. A 50-ohm CPW stub attached to the patch induces a phase modulation needed. Fig. 7 shows the phase modulation as a function of the open-ended and shorted stub length as simulated with Ansoft HFSS.

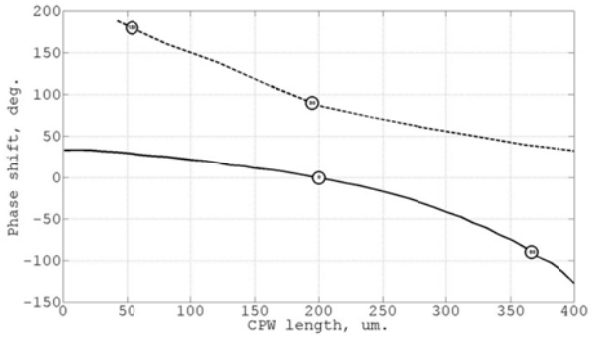

Figure 7. The relative phase of the back-reflected wavefront from element with open-ended (solid line) and shorted (dashed line) CPW stub.

A 200-µm open-ended stub is chosen as the zero-degree reference point, from which follows that 270° phase shift (−90° in Fig. 7) is achieved with a 366-µm open-ended stub. For shorted stub, the lengths are 195 µm and 54 µm, for +90° and +180° phase shift, respectively.

III. Reflectarray Performance

Array Element Efficiency

In addition to the modulated reflected field, also an unmodulated reflection occurs. This specular reflection reduces the efficiency as part of the illuminating power does not go to the steered beam. Array element efficiency can be defined as power ratio:

$$\eta_{element} = \frac{|E_m|^2}{|E_m|^2 + |E_0|^2}, \quad (3)$$

where E_m is the modulated part and E_0 is the unmodulated part of the reflected field.

The array element efficiency is simulated with Ansoft HFSS. A plane-wave excitation from direction normal to reflectarray elements is applied. The back-reflected field is simulated as a function of CPW stub length. Both open-ended and shorted stub are used in simulations. The back-reflected electric field is presented on the complex plane in Fig. 8 with the stub length from 0 µm to 400 µm as a parameter. The back-reflected electric field, $E_m + E_0$, lies on a circle in the complex plane. The origin of the circle represents the unmodulated part of the electric field, E_0, and the radius of the circle represents the absolute value of the modulated part of the back-reflected field, E_m. From Fig. 8 and Eq. (2), $\eta_{element} = 0.52$ and 0.64 for open-ended and shorted stub, respectively. Due to difference in the stub termination, the efficiency is different for open-ended and shorted stub. As a result, also the amplitude of the reflected field will be modulated.

The effects of non-ideal efficiency on the steered beam are presented in Fig. 9. The less-than-unity efficiency produces a wide beam around the specular direction. Also, using elements with both open-ended and shorted stubs creates an amplitude-modulating reflectarray, which produces a narrow beam even without phase modulation. Both unidealities are at level of −25 dB or less.

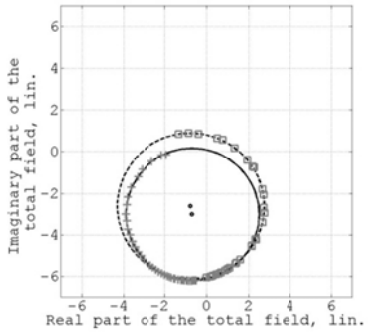

Figure 8. Simulated back-reflected electric field with open-ended (crosses) and shorted (squares) CPW stub, when the stub length is varied. The element efficiency is found by fitting a circle to data on the complex plane.

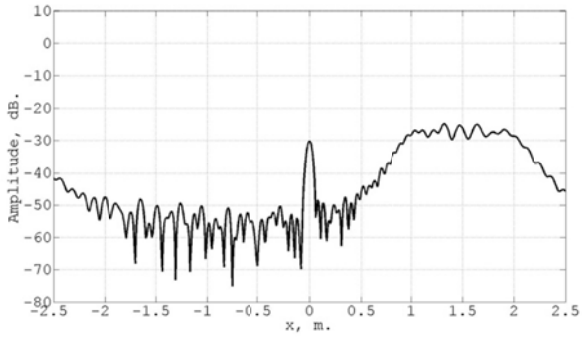

Figure 9. Reflected beam from a reflectarray without phase modulation. The specular reflection from the array structure produces a wide beam centered around 1500 m at 3000-mm distance. The amplitude modulation due to different stubs creates a narrow beam.

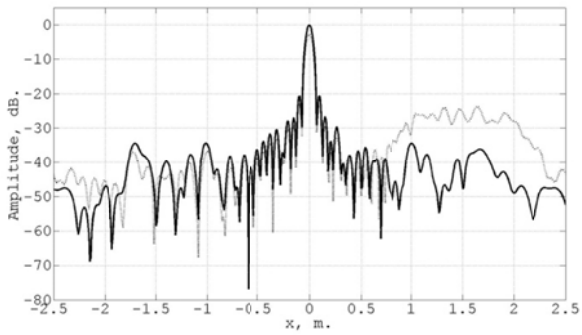

Figure 10. Beam from a reflectarray focused at $x = 0$ mm, $y = 0$ mm, $z = 3000$ mm with $\eta_{element}$ =1 (solid line) and $\eta_{element} = 0.52$ or 0.64 (dashed line) for open-ended or shorted stub, respectively.

Effect of Manufacturing Errors

Prior to manufacturing the 140-mm reflectarray, the effect of manufacturing errors are studied. The errors are related to the mechanical accuracy of the lithographic processing of the wafers. Two cases are considered: inaccuracy in

1. Polyimide substrate thickness, nominally 50 µm
2. CPW gap width, nominally 8 µm

Reflectarray element representing 0° state (open-ended 200-µm stub) is simulated with different parameters. In the simulation, CPW gap is varying from 6 µm to 10 µm and substrate thickness is varying from 40 µm to 60 µm, considered to represent realistic manufacturing inaccuracies. Fig. 11 presents the back-reflected electric field on the complex plane with different parameters.

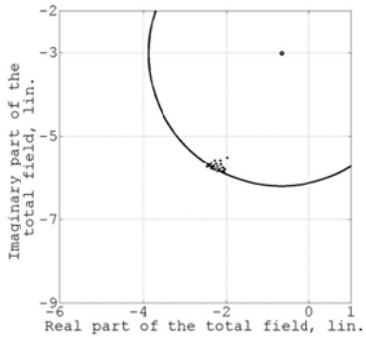

Figure 11. Simulated back-reflected electric field with open-ended 200-µm CPW stub, when CPW gap width and substrate thickness are varied.

Element efficiency and phase modulation with different parameted values are presented in Fig. 12. The values are relative to those with the nominal element. The phase modulation and efficiency deviates −4.0° … +3.5° and −11 % … +2.5 %, respectively.

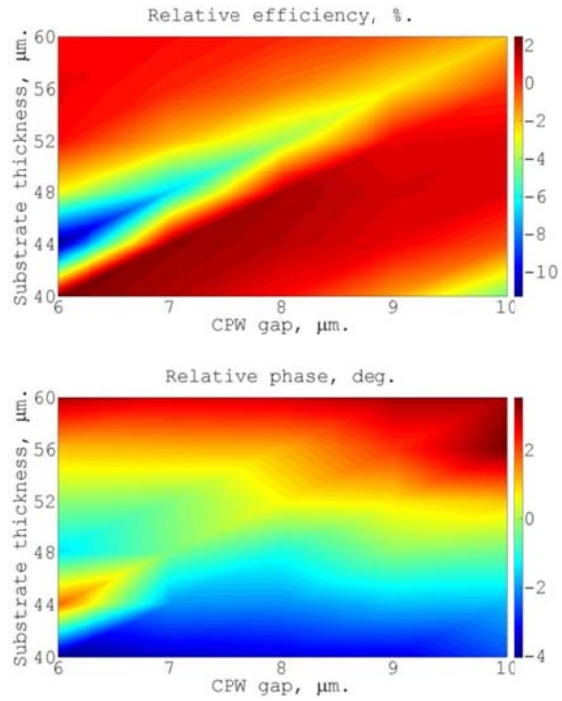

Figure 12. a) Efficiency and b) phase modulation as a function of element paremeters, the CPW gap width and substrate thickness.

IV. REFLECTARRAY MANUFACTURING

The actively controlled reflectarray will be manufactured on top of a high-voltage CMOS wafer. High voltages up to 50 V are needed todrive the MEMS phase shifters and they can be generated on-board using charge pump circuits. The wafer is composed of array tiles which can be sized 10 mm × 10 mm, 20 mm × 20 mm or 40 mm × 40 mm. It would be beneficial to keep the tile size smaller than the maximum size of the stepper exposure reticle which is about 20 mm × 20 mm.

When a reflectarray is composed of tiles, and when there are discontinuities between tiles, side lobes emerge according to the array pattern of the discontinuities. Figure 13 shows the simulated beam at 120 GHz for a 200 × 200 mm reflectarray consisting of 10 mm × 10 mm and 20 mm × 20 mm sub-array tiles with 2 mm wide gaps between the tiles. The diffraction lobes are below −12 dB and −17 dB for 10 mm × 10 mm and 20 mm × 20 mm tiles, respectively.

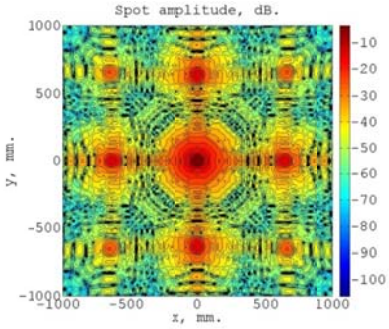

a)

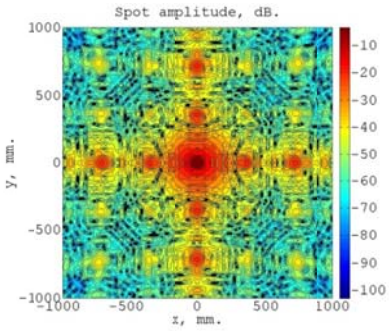

b)

Figure 13. Simulated beams at 120 GHz for a) 10 mm x 10 mm and b) 20 mm x 20 mm sub-array tiles.

A stackup of the reflectarray tile is presented in Fig. 14. The antennas and MEMS devices are built on top of a pre-processed Si-CMOS wafer. A HD4110 polyimide layer with a thickness of 50 μm is used as the dielectric substrate for the antennas. Metallised vias through the polymer are used to bring the control signals for the MEMS devices and also act as grounding vias for the GCPW antennas and feed lines.

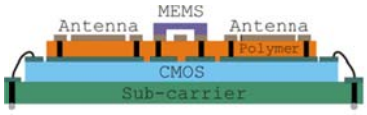

Figure 14. Reflectarray tile stackup.

The diced chips from the wafer are mounted on a slightly larger PCB sub-carrier and all connections are wire-bonded. The finalized array tiles are then mounted on a large carrier board using BGA techniques. The carrier board will have the outside interface, memory and FPGA address decoding circuits to handle the rapid beam scanning. Only the size of the carrier PCB will limit the maximum possible reflectarray size.

V. CONCLUSIONS

We have described design and presented simulation results for a 120-GHz reflectarray. Static reflectarrays are designed prior to an actively controlled MEMS-based reflectarray. Phase shifting patterns for 3713-element array are generated with an in-house genetic algorithm.

Reflectarray antenna element is characterized with simulations. The phase shifting elements, open-ended or shorted stubs, are optimized to provide 4-state phase shift. Also, the reflectarray efficiency is studied in order to find out power division between the controlled field and the specular reflection from the array surface. The less-than-unity and varying efficiency results in specular reflection from the array and introduces an unintended beam. Effect of manufacturing errors are simulated. Varying both the gap of the CPW and the substrate thickness results in maximum deviation of −11 % and −4° in efficiency and phase, respectively.

Finally, reflectarray manufacturing considerations for the actively controlled array are discussed. Unlike the single-wafer design with the static reflectarrays, the active array will be manufactured of identical subarrays. The subarray pattern can produce side lobes. Work is underway to find a design, which suffers least from this unideality.

ACKNOWLEDGMENT

This work has been partially supported by TEKES the Finnish Agency for Technology and Innovation, decision number, through SIMIDS project.

The first author Aleksi Tamminen wishes to thank Graduate School of Electronics, Telecommunication and Automation (GETA), Nokia Foundation, Finnish Foundation for Technology Promotion, Emil Aaltonen Foundation, and Association for Electronics Engineers for their financial support.

REFERENCES

[1] D. M. Pozar, S. D. Targonski, and H. D. Syrigos, “Design of millimeter wave microstrip reflectarrays,” *IEEE Transactions on Antennas and Propagation*, vol. 45, no. 2, pp. 287-296, February 1997.

[2] H. Kamoda, T. Iwasaki, J. Tsumochi, and T. Kuki, “60-GHz electrically reconfigurable reflectarray using p-i-n diode,” *Proceedings of International Microwaves Symposium*, Boston, MA, USA, June 2009, pp. 1177-1180.

[3] S. Montori, C. Fritzsch, L. Marcaccioli, R. V. Gatti, R. Jakoby, and R. Sorrentino, “Design and measurements of a 1-bit reconfigurable elementary cell for large electronic steerable reflectarrays,” *Proceedings of the 40th European Microwave Conference*, Paris, France, September 2010, pp. 918-921.

[4] J.M. Johnson and Y. Rahmat-Samii, “Genetic algorithms in engineering electromagnetics,” *IEEE Antennas Propagation Magazine*, vol. 39, no. 4, pp. 7-21, August 1997.

[5] D.S. Weile and E. Michielssen, "Genetic algorithm optimization applied to electromagnetics: A review," *IEEE Transactions on Antennas Propagation,* vol. 45, no. 3, pp. 343–353, March 1997.

[6] Y. Rahmat-Samii and E. Michielssen , "Electromagnetic optimization by genetic algorithms," John Wiley & Sons, Inc., New York, 1999.

[7] J. Huang and J.A. Encinar, "Reflectarray antennas," John Wiley & Sons, Inc., New Jersey, 2008.

[8] J. Huang and R. J. Pogorzelski, "A Ka-band microstrip reflectarray with elements having variable rotation angles," *IEEE Transactions on Antennas and Propagation*, vol. 46, no. 5, pp. 650–656, May 1998.

[9] M. Arrebola, J.A. Encinar, and M. Barba, "Multifed printed reflectarray with three simultaneous shaped beams for LMDS central station antenna," *IEEE Transactions on Antennas and Propagation*, vol. 56, no. 6, pp. 1518–1527, June 2008.

[10] C. Wan and J. A. Encinar, "Efficient computation of generalized scattering matrix for analyzing multilayered periodic structures," *IEEE Transactions on Antennas and Propagation*, vol. 43, no. 11, pp. 1233–1242, November 1995.